Cement and Concrete Research 40 (2010) 384–391

Contents lists available at ScienceDirect

Cement and Concrete Research

journal homepage: http://ees.elsevier.com/CEMCON/default.asp

Influence of clays on the rheology of cement pastes

Nathan A. Tregger *, Margaret E. Pakula, Surendra P. Shah

Northwestern University, Civil and Environmental Engineering, 2145 Sheridan Road, Evanston, IL 60208, USA

ARTICLE INFO

Article history:
Received 12 July 2008
Accepted 9 November 2009

Keywords:
Clay
Fresh concrete
Rheology
Cement paste
Flocculation

ABSTRACT

The fresh state of concrete is becoming increasingly important in furthering the types of applications of today's construction world. Processing techniques have resulted in technologies such as self-consolidating concrete and depend on the microstructural changes that take place during and immediately after mixing and placing. These changes to the microstructure reflect the flocculation behavior between the particles in suspension. The ability to modify this behavior allows control over the balance among flowability and shape-stability of concrete. This study investigates how clay admixtures affect the microstructure of cement pastes from a rheological stand point. Shear and compressive rheology techniques are used to measure how the solids volume fraction of suspensions with different admixtures evolves with stress. Based on these relationships, the effectiveness of clays on the balance between flowability and shape-stability is measured. Results are consistent with green strength tests performed on concrete mixes derived from the cement paste mixes.

1. Introduction

The fresh state of concrete is becoming increasingly important in advancing the types of applications of today's construction world. Processing techniques have resulted in technologies such as self-consolidating concrete (SCC) and depend on the microstructural changes within concrete during the first hours after mixing and placing. The ability to modify the microstructure has led to high-performance concretes such as SCCs with reduced formwork pressure [1], and minimal-compaction energy concrete for slipform paving applications [2,3]. Minimal-compaction energy concrete requires sufficient flowability in order to consolidate without the use of internal vibration. However, this concrete must also gain sufficient shape-stability in order to keep its shape immediately after slipform paving; a process which involves consolidation and extrusion. It has been demonstrated for minimal-compaction energy concrete that small additions of clays (less than 1% by mass of cement) have made substantial improvements on the shape-stability. Similarly, clays have also been shown to improve the cohesiveness of cement-based extruded materials at very low dosages [4,5].

The purpose of this study is to quantify how clay admixtures affect the strength of the microstructure from a rheological stand point. Shear and compressive rheology techniques are used to measure how the solids volume fraction of cement suspensions with different admixtures evolves with stress. Based on these relationships, the effectiveness that clays and other admixtures have on the balance between flowability and shape-stability can be measured. A shear rheology method [6] is used to investigate how the maximum solids volume fraction of the flocs changes under shear stress, while a compressive rheology method [7] is used to determine changes in the local solids volume fraction (solids volume fraction of the sediment region) under compressive stress. Results are consistent with green strength tests performed on concrete mixes derived from the cement paste mixes investigated.

2. Background

When water and cement are combined in typical proportions, the inherent high solids concentration of the paste leads to the rapid formation of flocs rapidly due to the increase in the frequency of particle collisions [8]. During mixing, there is a constant formation and breakage of flocs. For a constant mixing speed, the floc size will reach an equilibrium that is a function of the flocculation strength; higher flocculation strengths can sustain larger flocs [9]. At sufficiently high mixing rates, the microstructure will reach a maximum solids volume fraction or maximum packing density that is a function of the flocculation strength as well as the particle size distribution and shape [10]. For suspensions with similar particle size distributions and shapes, stronger floc strengths lead to lower maximum packing densities.

Once mixing is complete, the flocs are free to grow, forming a space-filling network capable of supporting stress. The rate at which this occurs depends on both the rate of successful collisions, and the rate of breakage due to particle movement arising from Brownian motion and settling action [11].

The fresh cement paste microstructure can sustain shear stresses elastically up to the yield stress. The yield stress is dependent on both the flocculation strength and structure of the suspension [12]. When the shear stress exceeds the yield stress, flow is initiated and flocs

* Corresponding author. 2145 Sheridan Road, Suite A130, Evanston IL, 60208. Tel.: +1 847 491 7161.
E-mail address: n.tregger@u.northwestern.edu (N.A. Tregger).

0008-8846/$ – see front matter © 2009 Elsevier Ltd. All rights reserved.
doi:10.1016/j.cemconres.2009.11.001

begin to break down into smaller flocs. This microstructural process releases entrapped liquid within the flocs, increasing the liquid available for lubrication between particles. As a result, the viscosity decreases with increased shear, which explains the shear-thinning behavior of suspensions such as cement pastes [13,14].

Cement paste responds in a thixotropic manner when shear stresses are applied and removed; flocs break apart under stress, leading to a decrease in viscosity, but rebuild over time once the stress is removed, subsequently increasing the viscosity [15]. This reversible property is essential to the fresh state of concrete and has garnered much research in recent years [16–21]. Thixotropy is especially convenient for applications such as formwork pressure, where the increase in viscosity over time leads to a decrease in formwork pressure [22–24]. The influence of clays on thixotropy will be assessed in future work, but is not investigated here; the main focus is the effect of clays on floc strength.

The concept of a yield stress exists in suspensions subjected to compression just like suspensions subjected to shear stress. Below the yield stress, a suspension will deform elastically, and when the yield stress is exceeded, the microstructure will irreversibly collapse, where flocs break apart in order to rearrange into a denser configuration. As the flocs break apart, entrapped liquid is released, and the slow migration of water through the dense microstructure results in a viscoelastic response [25]. This new, denser configuration will in turn have a higher yield stress, since more particles must rearrange themselves to allow for further consolidation.

3. Theoretical background for data analysis

3.1. Shear rheology test method

In studies by Soua et al. and Liu [6,9], methods were developed to estimate the relative floc size of highly-concentrated suspensions for a given shear stress. For non-flocculated suspensions, the well-known Krieger and Dougherty model [26] relates the viscosity of a suspension to the volume fraction by Eq. (1):

$$\frac{\eta}{\eta_0} = \left(1-\frac{\phi}{\phi_m}\right)^{-K}, \tag{1}$$

where η is the viscosity of the suspension, η_0 is the viscosity of the suspending medium, ϕ is the volume fraction, ϕ_m is the maximum packing density and K is a fitting parameter, usually taken as 2, determined from experiments. Stuble and Sun [27] demonstrated that the Krieger and Dougherty model could be fitted for cement pastes, even if the parameters in Eq. (1) do not take on the same physical meanings as those for a non-flocculated, suspensions [27,28]. This model implies that an increase in viscosity is due to an increase in solids volume, and furthermore, as $\phi \to \phi_m$, $\eta \to \infty$. A convenience of having K fixed as 2 is that the maximum packing fraction can be determined by fitting a straight line to $1-(\eta/\eta_0)^{-1/2}$ versus ϕ; when $1-(\eta/\eta_0)^{-1/2}$ approaches 1, ϕ_m is achieved. However, flexibility is lost in the ability to fit the data to experiments. In order to increase the flexibility, Liu [10] added an adjusting parameter to yield Eq. (2):

$$\frac{\eta}{\eta_0} = \left[b\left(1-\frac{\phi}{\phi_m}\right)\right]^{-2} = [a(\phi_m-\phi)]^{-2}, \tag{2}$$

where the adjusting factor $a = b/\phi_m$. Soua et al. extend this concept to account for flocculated suspensions (in a similar fashion to a study by Liu [9]) [6]. As flocs form, they begin to trap water, reducing the amount of free water available to lubricate the system. As a result, the viscosity of the suspension increases. Furthermore, Eq. (2) does not hold, and the relationship between viscosity and volume fraction becomes a relationship between viscosity and effective volume fraction (floc volume fraction). This effective volume fraction accounts for the increase of entrapped water. Similarly, the maximum packing fraction varies with stress for a given floc size.

As the evolving flocs are subjected to increasing shear stress, the flocs will break down in size and continue to do so until the individual particles are achieved. Fig. 1 demonstrates how the maximum packing density of the flocs (ϕ_{fm}) evolves with stress. As the stress increases, the flocs begin to break down and release entrapped water resulting in a decrease in viscosity. In addition, particles can realign within the flow field to form a tighter configuration [6]. When the stress is sufficiently larger than the yield stress, ϕ_m is approached and all the entrapped water from the flocs is released. As a result, Eq. (2) now becomes Eq. (3) according to Soua et al. [6]:

$$\frac{\eta}{\eta_0} = \left[b\left(1-\frac{\phi_f}{\phi_{fm}}\right)\right]^{-2} = [a'(\phi_{fm}-\phi_f)]^{-2} \quad \text{for } \tau > \tau_y, \tag{3}$$

where ϕ_f is the volume fraction of the flocs, ϕ_{fm} is the maximum packing density of the flocs and $a' = b/\phi_{fm}$, τ is the shear stress and τ_y is the yield stress of the suspension. Note that for $\tau \gg \tau_y$, Eq. (3) becomes Eq. (4) [similar to Eq. (2)]:

$$\frac{\eta}{\eta_0} = [a(\phi_m-\phi)]^{-2} \quad \text{for} \quad \tau \gg \tau_y. \tag{4}$$

In order to determine ϕ_{fm} and ϕ_m, a method developed by Liu can be implemented [10]. Flow curves are obtained for different initial volume fractions. For each stress value of each curve, the apparent viscosity, η, is calculated by taking the slope (stress / strain rate), shown in Fig. 2, marked by the circles for an example stress of 68 Pa. Then, for each stress value, the value $1-(\eta/\eta_0)^{-1/2}$ is plotted against the corresponding volume fraction. A linear fit is then applied and when $1-(\eta/\eta_0)^{-1/2}=1$, the ϕ_{fm} is achieved for that given stress value, as shown in Fig. 3. Repeated for each stress value gives a ϕ_{fm}–τ curve. Finally, ϕ_m is the ϕ_{fm} value for $\tau \gg \tau_y$ of the curve. For example, Fig. 4 shows ϕ_{fm}/ϕ_y versus τ/τ_y (where ϕ_y is ϕ_{fm} at τ_y), for a plain cement paste representing a flocculated suspension and a cement paste containing a high-range water-reducer representing a deflocculated suspension. Although ϕ_m is primarily dependent on the particle size distribution and shape, a flocculated suspension typically shows a lower ϕ_m when compared to a deflocculated system [27,29–31], which is demonstrated in Fig. 4. In addition to the ϕ_m, the difference between ϕ_m and ϕ_y (or ϕ_{dif}) is less than the deflocculated mix; that

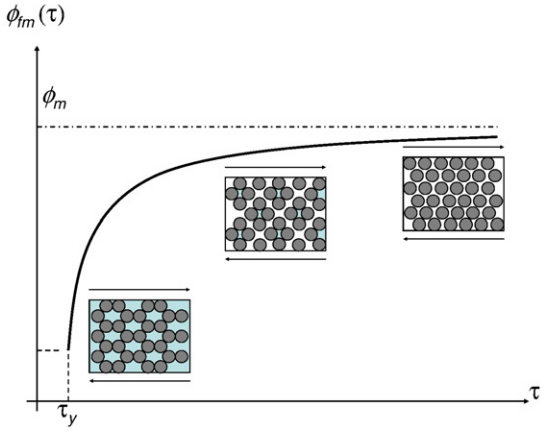

Fig. 1. Evolution of maximum packing density of flocs as a function of stress.

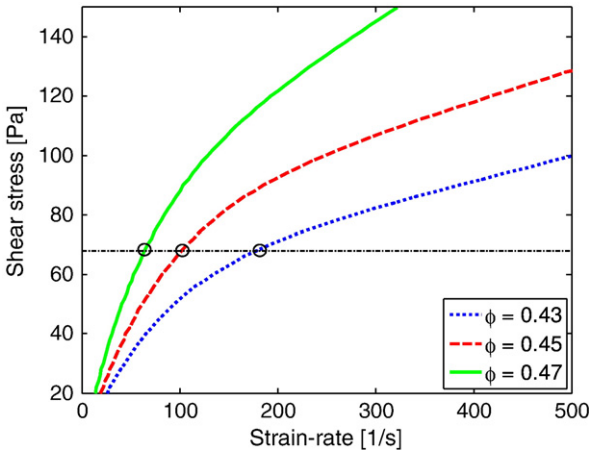

Fig. 2. Flow curve depicting circles where viscosities are calculated for a given stress value.

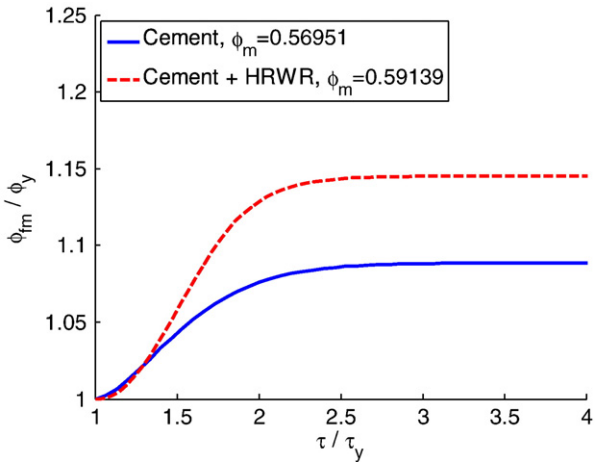

Fig. 4. Shear rheology method comparisons between cement pastes with and without a high-range water-reducer.

is, the structure changes less with increasing stress. This can be considered as another indication of floc strength.

3.2. Compressive rheology method

When the yield stress is exceeded in compression, the suspension's network collapses irreversibly, leading in a denser configuration. The increase in the local solids volume fraction results in a higher compressive yield stress in the new configuration, since a denser configuration requires more particles to rearrange themselves to allow further consolidation. Thus, the compressive yield stress is a function of the local solids volume fraction, and is governed by the particle arrangement and strength of the microstructure. In general, a higher number of contact points between flocs or the stronger bonds between flocs will increase the yield stress. However, the level of heterogeneity of the microstructure can also play a role [see for example, [32]].

The compressive yield stress can be determined experimentally in several different ways, and in this study, the centrifugal approach is used [7]. In this method, a suspension is subjected to different accelerations as sketched in Fig. 5. At each acceleration, the equilibrium height of the sediment region is recorded. This set of data, along with the density, initial volume fraction and centrifuge characteristics are analyzed to determine the compressive yield stress. Both the yield stress and local solids volume fraction are solved from Eq. (5) which is derived from force balance and continuity equations [33]:

$$\frac{dP}{dz} = -\Delta\rho g \phi_0 \left(1 - \frac{z}{R}\right), \tag{5}$$

where P is the pressure, z is the distance from the bottom of the centrifuge specimen tube, $\Delta\rho$ is the density difference between solid and liquid phases, g is the centrifugal acceleration, ϕ_0 is the initial volume fraction, and R is the distance between the center of the centrifuge and the bottom of the centrifuge specimen tube (see Fig. 5). Solving this equation requires a numerical integration scheme. The theory is described in [33], and an approximate solution is given in [7,33]. This approximation (which was used in this study) applies the mean value theorem to the conservation of mass condition, bypassing numerical integrations and cumbersome iterative processes, yet sacrificing little accuracy [33]. The solution includes equations for the pressure and volume fraction at the bottom of the centrifuge tube [Eqs. (6) and (7)]:

$$P(bottom) \cong \Delta\rho \phi_0 H_0 g \left(1 - \frac{H_{eq}}{2R}\right), \tag{6}$$

$$\phi(bottom) \cong \frac{\phi_0 H_0 \left[1 - \frac{1}{2R}\left(H_{eq} + g\frac{dH_{eq}}{dg}\right)\right]}{\left[\left(H_{eq} + g\frac{dH_{eq}}{dg}\right)\left(1 - \frac{H_{eq}}{R}\right) + \frac{H_{eq}^2}{2R}\right]}, \tag{7}$$

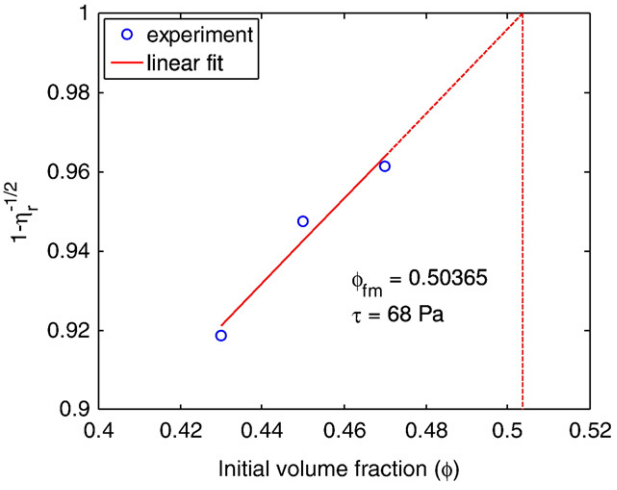

Fig. 3. Determination of maximum packing density of the flocs.

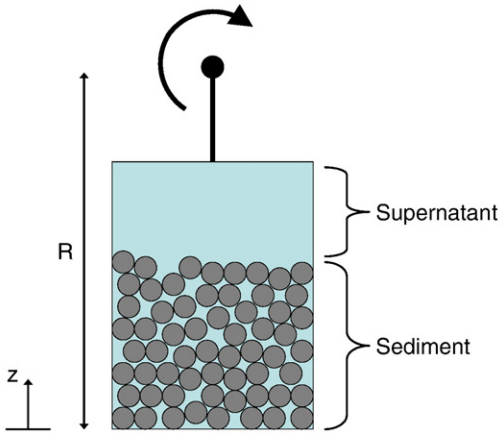

Fig. 5. Schematic of centrifuge process.

where H_0 is the initial height in the centrifuge tube and H_{eq} is the equilibrium height at the given acceleration. $P(bottom)$, the compressive yield stress at the bottom of the tube, can then be plotted as a function of $\phi(bottom)$, the local volume fraction at the bottom of the tube, for a series of equilibrium heights corresponding to different accelerations. Among many other dense suspensions, this method has been successfully used for cement mixes [34]. For mixes with similar particle arrangements, a higher compressive yield stress for a particular local solids volume fraction represents a higher flocculation strength as shown in Fig. 6, where a plain cement paste is compared to a cement paste containing a high-range water-reducer.

4. Experimental methods and materials

In this study, six different mix compositions were tested: a cement control mix (CM), a cement-fly ash mix (FA), a cement-high-range water-reducing mix (HW) and three different cement–clay mixes (C1, C2, and C3). The descriptions of the solids are shown in Table 1. All three clays are commercially available. C1 is a highly purified, magnesium alumino silicate. The purification process involves a wet exfoliation of high water demand impurities such as smectite [35]. Under shearing, C1 breaks down into needle like structures with a length on the order of a micron but a diameter on the order of several nanometers. C2 is a kaolinite clay that has typically been used to modify rheological behaviors in cement and concrete [36]. C3 is a metakaolin clay, composed of pozzolonic amorphous alumino silicates formed by controlled calcination of kaolinite. The particle size distribution is finer than fly ash particles, yet coarser than silica fume particles. This leads to improved reactivity over fly ash, and reduced water demand compared to silica fume [37]. A naphthalene-based high-range water-reducing admixture was also used.

4.1. Mix designs and mix protocol

Concerning the shear rheology method, three different volume fractions were required to determine the maximum packing density relationship: 0.43, 0.45 and 0.47. Each different composition was subjected to the same range of volume fractions, keeping the admixture-to-cement ratio constant. For the compressive rheology method, all mixes had the same initial solids volume fraction of 0.45, which corresponds to a w/b of about 0.40 for the control mix. The mix designs are shown in Tables 2–4, while the mixing protocol is shown in Table 5. A small planetary mixer was used. It is noted that the dry ingredients were mixed first in order to achieve proper dispersion of the mineral admixtures before the water was added. For dense suspensions such as cement pastes, flocculation occurs rapidly, which can hinder proper dispersion before the microstructure is formed.

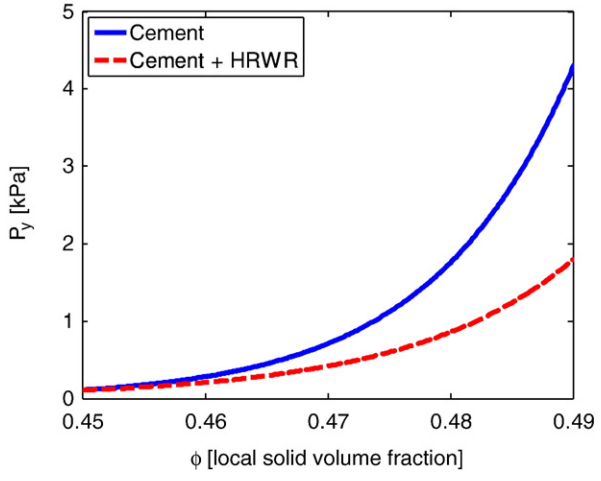

Fig. 6. Comparison of compressive yield stresses between cement pastes with and without a high-range water-reducer.

Table 1
Description of solid materials.

Material	Particle size, μm (μ in)	Description
Cement (CM)	14.8 (582)	Type I
Fly ash (FA)	23.5 (925)	Class C
Clay 1 (C1)	65.2 (2567), 1.75[a] (68.9)[a]	Purified magnesium alumino silicate
Clay 2 (C2)	13.0 (512), 0.50[a] (19.7)[a]	Kaolinite, illite, quartz
Clay 3 (C3)	3.54 (139), 1.20[a] (47.2)[a]	Purified calcined kaolinite

[a] Highly dispersed state.

4.2. Shear rheology method

A temperature-controlled rheometer with a coaxial cylinder geometry was used to determine the flow curves for the shear rheology method. The protocol involved a 2 min pre-shear at 300 s^{-1} followed by 2 min of rest. The strain rate was then increased gradually over 10 min to a final value of 200 s^{-1}. Flow curve results included shear stress versus strain-rate curves. This was performed for each volume fraction three times each on nominally identical mixes. From this data, $1-(\eta/\eta_0)^{-1/2}$ versus ϕ was plotted and these curves were extrapolated to 1 for each shear stress in order to determine the maximum packing density. The ϕ_{fm} relationship was then constructed to find ϕ_m.

4.3. Compressive rheology method

A superspeed centrifuge was used to determine the compressive yield stress as a function of the local solids volume fraction. In order to achieve a flat bottom, the centrifuge tubes were filled with a structural epoxy. After mixing, four samples of the same batch were centrifuged simultaneously for 20 min at each speed. This was determined to be the minimum time required to ensure all specimens reached their equilibrium states. Equilibrium heights were obtained for rotational

Table 2
Mix design for a volume fraction of 0.43.

Material	Control (CM)	High-range water-reducer (HW)	Fly ash (FA)	Clay 1 (C1)	Clay 2 (C2)	Clay 3 (C3)
Cement, g	1350	1350	852	1334	1333	1334
Water, g	570	564	570	570	570	570
Admixture, g	0	6.8	365	13.3	13.3	13.3

Table 3
Mix design for a volume fraction of 0.45.

Material	Control (CM)	High-range water-reducer (HW)	Fly ash (FA)	Clay 1 (C1)	Clay 2 (C2)	Clay 3 (C3)
Cement, g	1413	1413	891	1396	1395	1396
Water, g	550	544	550	550	550	550
Admixture, g	0	7.1	382	14.0	14.0	14.0

Table 4
Mix design for a volume fraction of 0.47.

Material	Control (CM)	High-range water-reducer (HW)	Fly ash (FA)	Clay 1 (C1)	Clay 2 (C2)	Clay 3 (C3)
Cement, g	1476	1476	931	1458	1457	1458
Water, g	530	524	530	530	530	530
Admixture, g	0	7.4	399	14.6	14.6	14.6

Table 5
Mix protocol for cement compositions.

Time	Procedure
0:00	Mix dry ingredients on low speed
1:00	Add wet ingredients, continue mixing on low speed
3:00	Stop mixing, scrap edges of mixer
4:00	Mix on high speed
6:30	Stop mixing, scrap edges of mixer
7:30	Mix on high speed
10:00	End of mixing

Table 6
Mix protocol for concrete compositions.

Time	Procedure
0:00	Mix dry ingredients including fine aggregate on low speed
1:00	Add wet ingredients, continue mixing on low speed
3:00	Stop mixing, scrap edges of mixer
4:00	Mix on high speed
6:30	Stop mixing, scrap edges of mixer
7:30	Mix on high speed
10:00	Mix coarse aggregate on high speed
12:00	End of mixing

speeds ranging from 2000 to 10,000 rpm for each specimen. An example of the raw data is shown in Fig. 7, along with a theoretical fit. A regression analysis was performed to fit the data to an equation of the form:

$$\ln H_{eq} = a_1 + a_2 \ln g + a_3 (\ln g)^2, \tag{8}$$

as recommended by Green et al. [33], where the values a_1 through a_3 are the fitting parameters. From the data collected, Eqs. (6) and (7) could be used to determine the compressive yield stress.

4.4. Determination of green strength

In addition to the rheology methods, the green strength or strength immediately after casting was determined. These tests were performed on concrete mixes derived from cement pastes used in the previous tests. A coarse aggregate to fine material ratio of 1.75 and a fine aggregate to fine material ratio of 1.56 were used for all concrete mixes. The coarse aggregate consisted of a round pea gravel with a maximum size of 10 mm while the fine aggregate consisted of a river sand with a maximum size of 4.75 mm. After using the mixing protocol shown in Table 6, a 100×200 mm (4×8 in) cylinder was filled with concrete and then subjected to twenty-five drops on a drop table shown in. These drops represent external energy to help consolidate the mix. After consolidation, the fresh concrete was demolded and a bucket was placed on top of the fresh concrete cylinder. Sand was incrementally added until the cylinder collapsed. This load was then converted to green strength by dividing the original cross section. This process was repeated three times for each composition and is shown in Fig. 8.

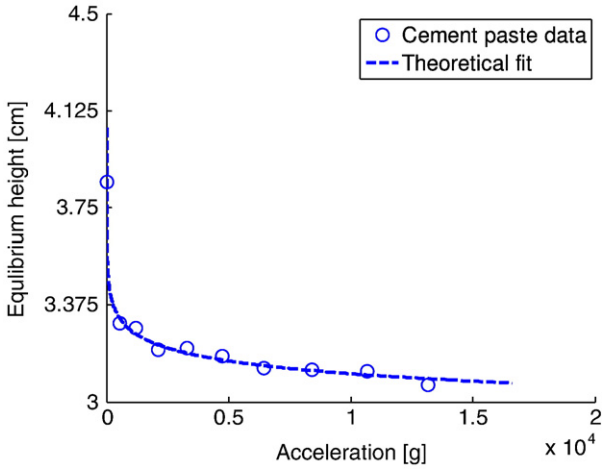

Fig. 7. Raw data from centrifuge for cement paste.

5. Results and discussion

Flow curves for each mix were fitted according to a modified Bingham equation given by [38]:

$$\tau = \tau_y \left[1 - \exp\left(3^{\dot{\gamma}}/_{\dot{\gamma}_{crit}}\right)\right] + \mu\dot{\gamma}, \tag{9}$$

where τ is the shear stress, τ_y is the yield stress, μ is the plastic viscosity, $\dot{\gamma}$ is the strain-rate and $\dot{\gamma}_{crit}$ is the critical strain rate corresponding to the yield stress. A modified Bingham equation was used because of its consistent ability to fit the experimental data. Table 7 gives the yield stress for the $\phi = 0.45$ mix, ϕ_y, ϕ_m and ϕ_{dif}. Fig. 9 shows the percent difference between these values as compared to the control cement mix. It can be seen that all the mixes have relatively the same ϕ_y, which is reasonable since only small dosages of additives were used except in the case of the FA mix (which has the largest difference compared to CM). However, the yield stresses for the HW and FA mixes are lower than CM while the C1–3 mixes are higher. This may indicate that although the compositions have similar structures, the bonds between flocs may be weaker for the HW and FA mixes, but stronger for the C1–3 mixes. As the stress increases, both ϕ_m and ϕ_{dif} are larger for HW and FA but smaller for C1–3. This also indicates larger floc strengths for mixes containing clays, and smaller floc strengths for mixes containing high-range water-reducer or fly ash. Fig. 10 shows ϕ_{fm} / ϕ_y versus τ /τ_y for all the compositions with their ϕ_m values listed. As noted by both Stuble and Sun and Mansoutre et al., the maximum packing density increases with stress [27,29]. Graphically, it is shown that the clay mixes do not change as much as the FA and HW mixes, indicating higher floc strengths. Struble and Sun used the traditional method of determining ϕ_m by fitting the

Fig. 8. Green strength test.

Table 7
Shear rheology results.

Mix	τ_y [Pa]	τ_y [psf]	ϕ_{min}	ϕ_m	ϕ_{dif}
CM	76.32	1.59	0.523	0.570	0.0465
HW	62.24	1.30	0.516	0.591	0.0750
FA	34.76	0.73	0.494	0.579	0.0853
C1	97.31	2.03	0.520	0.546	0.0255
C2	80.65	1.68	0.522	0.549	0.0268
C3	89.02	1.86	0.516	0.556	0.0397

Krieger and Dougherty model to ϕ–μ data. They reported ϕ_m values of 0.76 and 0.64 for cement pastes with and without high-range water-reducers respectively [27]. In this study, cement pastes with and without high-range water-reducers produced ϕ_m values of 0.59 versus 0.57. The differences in values may be due to slightly different chemical composition and particle size distribution. As for the smaller difference between the cement paste with and without high-range water-reducers, the most likely reason is that the high-range water-reducer mix was not fully dispersed as in the case for Struble and Sun [27]. As a further comparison, Mansoutre et al. also used a method similar to Struble and Sun to determine ϕ_m for C_3S pastes (the main reactive component in cement) and found ϕ_m to be around 0.45 [29].

The results for the compressive rheology method are shown in Fig. 11 as the relationship between the local solids volume fraction and compressive yield stress. Both the HW and FA mixes are more compressible compared to the CM mix. On the other hand, the mixes C1–3 all show a higher compressive yield stress CM. This further confirms the increase in floc strength of the C1–3 mixes while a decrease in the floc strength of HW and FA.

Naphthalene-based high-range water-reducers have been shown to increase the magnitude of the repulsive potential, resulting in weaker flocs [39–42]. Because the flocs are held loosely together, they can be easily broken down and rearranged under both shear and compressive forces. Using a different centrifuge method (that is capable of giving similar results to the centrifuge method used in this study [43])), Kjeldsen et al. demonstrate how high-range water-reducers in general reduces the compressive yield stress because of electrostatic and steric repulsion [42]. For the fly ash mix, improvements in flowability are usually attributed to the shape of the fly ash particles. The spherical shape of the fly ash particles minimizes surface area to volume ratio thus decreasing water demand. In addition, it is usually noted that the spherical shape acts as a ball bearing, allowing particles to easily roll over each other when rearrangement of the microstructure is required [44–48]. This would explain the low compressibility. Under high shear stresses, the fly ash can still achieve high volume fractions since the spherical shape and low water demand allow efficient flowability.

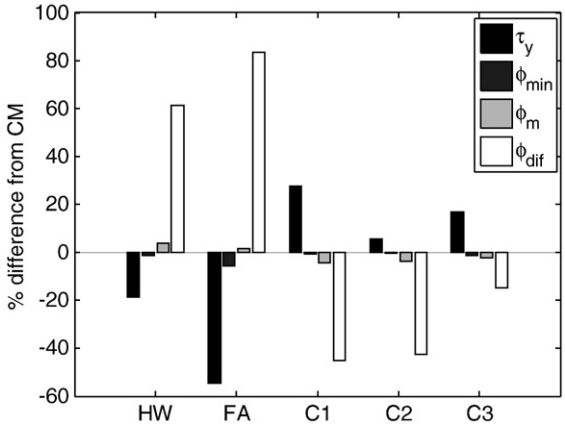

Fig. 9. Comparison of shear rheology results to control cement mix.

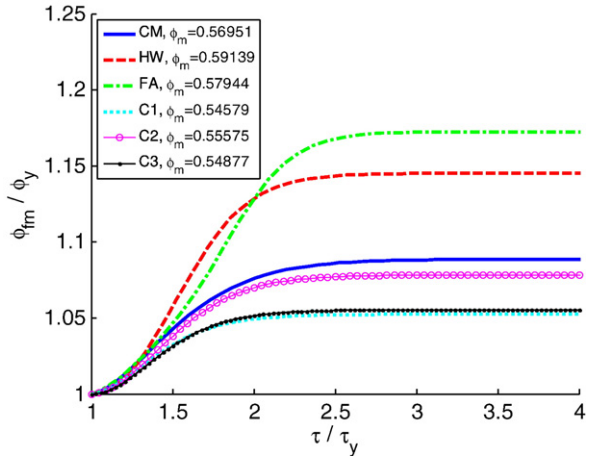

Fig. 10. Maximum packing densities as a function of stress.

When comparing the fly ash mix with the rest of the mixes used in the study, it should be noted that the microstructure of the fly ash mix may have a different particle size distribution since a large amount of cement was replaced with fly ash, where as only small amounts of admixtures were used in the other mixes.

As previously stated, for the clays, the shear rheology results show that although the ϕ_y values were similar to the CM mix, the τ_y, values were increased while the ϕ_m and ϕ_{dif} values were decreased. This suggests that the bonds between the particles are stronger. In addition, the compressive yield stresses are also higher for the clays than the control cement mix. One possible explanation of the larger floc strength is that the clays are absorbing water that would normally help lubricate the microstructure and allow particles to easily slide past each other during shear or compression. In the absence of this lubricating water, the suspension would have a higher shear and compressive yield stress. Yet, clays used in this study have all been processed to remove major impurities that are typically responsible for swelling usually associated with natural clays. In addition, the small clay dosages considered would further reduce the amount of water absorbed.

Another possibility is that the smaller clay particles are filling the interstices created by the larger cement particles. The number of physical contact points would increase leading to a larger compressive yield stress. However, a 1% addition of any clay type would not significantly improve the compressive strength. In other words, the small addition of clay does not dramatically change the geometry of

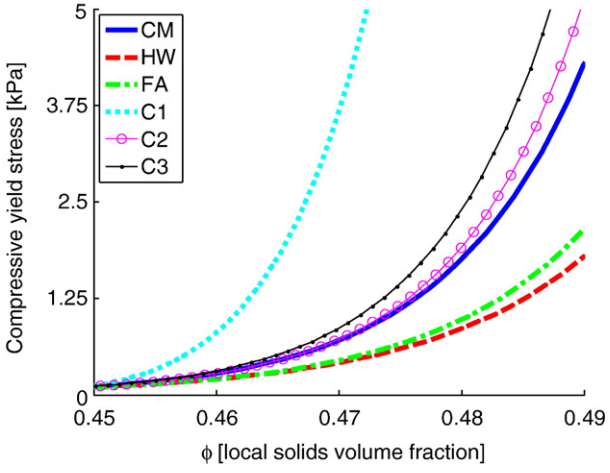

Fig. 11. Compressive rheology results.

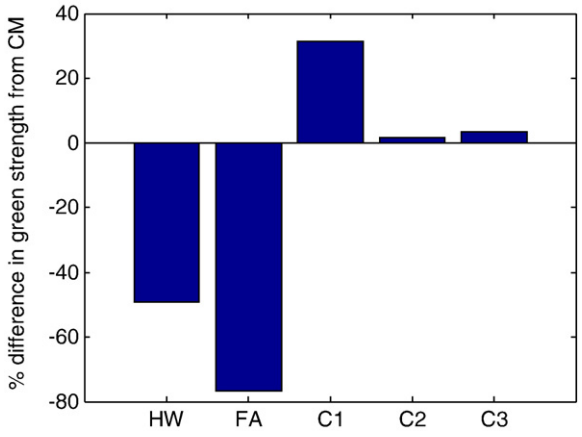

Fig. 12. Green strength results.

the floc arrangement (also noted by the similar ϕ_y values). Therefore, it is likely that with small dosages of clays, the shear and compressive yield stresses are increased due to an increase in the flocculation strength of the suspension. The exact nature of how clays increase the flocculation strength of cement pastes from a chemistry point of view was not within the scope of this paper.

Shape-stability of the fresh concrete is shown in Fig. 12 and Table 8 as determined by the green strength. The results are shown as the percent difference from the green strength of the control plain cement mix. Both the high-range water-reducer (HW) and the fly ash (FA) decrease the green strength compared to the plain cement mix (CM). On the other hand, all of the clays (C1, C2, C3) increase the green strength with C1 having the best efficiency. When comparing the shear rheology, compressive rheology and green strength tests, all agree that high-range water-reducing admixture and fly ash mixes decrease the tested values, while the clays increase them. In addition, the results also agree in the relative effectiveness of the clays with C1 performing the best.

6. Conclusions

Both shear and compressive rheologies can give helpful insight into how green strength is affected by different admixtures. Agreement was found between both shear and compressive rheologies and green strength tests performed on cement paste and concrete with the same matrix. The results show how both the high-range water-reducing admixture and fly ash decrease the shear and compressive strength based while the clays increase the shear and compressive strength. Clays showed a lower maximum packing fraction as well as a smaller change in packing fraction while the HW and FA showed opposite trends. It was shown that the nanoclay, C1, a purified magnesium alumino silicate clay, was most effective in improving the shape-stability.

Information from these tests shows a direct connection between micro and macro behaviors and specifically flocculation strength and green strength. Future progress in the concrete industry can be made by altering nano properties of admixtures to improve flocculation behaviors, creating superior concretes with tailored, fresh-state properties.

Table 8
Green strength results.

	Green strength [kPa]	Green strength [ksf]
CM	14.80	0.3090
HW	7.52	0.1570
FA	3.47	0.0724
C1	19.44	0.4060
C2	15.04	0.3141
C3	15.30	0.3196

Acknowledgements

The authors would like to acknowledge the financial support from both the Infrastructure Technology Institute at Northwestern University and the Center for Portland Cement Concrete Pavement Technology at Iowa State University.

References

[1] R. Ferron, A. Gregori, Z. Sun, S.P. Shah, Rheological method to evaluate structural buildup in self consolidating concrete cement pastes, ACI Materials Journal 104 (3) (2007) 242–250.
[2] B.Y. Pekmezci, T. Voigt, K. Wang, S.P. Shah, Low compaction energy concrete for improved slipform casting of concrete pavements, ACI Materials Journal 104 (3) (2007) 251–258.
[3] N. Tregger, T. Voigt, S.P. Shah, Improving the slipform process via material manipulation, in: C.U. Grosse (Ed.), Advances in Construction Materials 2007, Springer Berlin Heidelberg, New York, 2007, pp. 539–546.
[4] K. Kuder, S.P. Shah, Rheology of extruded cement-based materials, ACI Materials Journal 104 (3) (2007) 283–290.
[5] T. Voigt, T. Malonn, S.P. Shah, Green and early age compressive strength of extruded cement mortar monitored with compression tests and ultrasonic techniques, Cement and Concrete Research 36 (5) (2006) 858–867.
[6] Z. Soua, O. Larue, E. Vorobiev, J.L. Lanoisellé, Estimation of floc size in highly concentrated calcium carbonate suspension obtained by filtration with dispersant, Colloids and Surfaces A 274 (1–3) (2006) 1–10.
[7] R. Buscall, L.R. White, On the consolidation of concentrated suspensions I: the theory of sedimentation, Journal of Chemical Societies Faraday Transactions 83 (3) (1987) 873–891.
[8] P. Jarvis, B. Jefferson, J. Gregory, S.A. Parsons, A review of floc strength and breakage, Water Research 39 (14) (2005) 3121–3137.
[9] D.M. Liu, Theoretical determination of floc size in highly-concentrated zirconia-wax suspensions, Acta Materialia 50 (8) (2002) 1927–1935.
[10] D.M. Liu, Particle packing and rheological property of highly-concentrated ceramic suspensions: ϕ_m determination and viscosity prediction, Journal of Materials Science 35 (21) (2000) 5503–5507.
[11] D.N. Thomas, S.J. Judd, N. Fawcett, Flocculation modeling: a review, Water Research 33 (7) (1999) 1579–1592.
[12] S.B. Johnson, G.V. Franks, P.J. Scales, D.V. Boger, T.W. Healy, Surface chemistry–rheology relationships in concentrated mineral suspensions, International Journal of Mineral Processing 58 (1–4) (2000) 267–304.
[13] G.H. Tattersall, P.F.G. Banfill, The Rheology of Fresh Concrete, Pitman Advanced Publishing Program, Boston, 1983.
[14] R. Shaughnessy, P.E. Clark, The rheological behavior of fresh cement pastes, Cement and Concrete Research 18 (1988) 327–341.
[15] H.A. Barnes, Thixotropy — a review, Journal of Non-Newtonian Fluid Mechanics 70 (1–2) (1997) 1–33.
[16] R. Ferron, A. Gregori, Z. Sun, S.P. Shah, Rheological method to evaluate the thixotropy of cement pastes for SCC, ACI Materials Journal 104 (2) (2007) 242–250.
[17] N. Roussel, Steady and transient flow behavior of fresh cement pastes, Cement and Concrete Research 35 (9) (2005) 1656–1664.
[18] S. Jarny, N. Roussel, R. LeRoy, P. Coussot, Modelling thixotropic behavior of fresh cement pastes from MRI measurement, Cement and Concrete Research 38 (5) (2008) 616–623.
[19] J. Assaad, K.H. Khayat, H. Mesbah, Assessment of thixotropy and self-consolidating concrete, ACI Materials Journal 100 (2) (2003) 99–107.
[20] J.E. Wallevik, Rheological properties of cement paste: thixotropic behavior and structural breakdown, Cement and Concrete Research 39 (1) (2009) 14–29.
[21] D.A. Williams, A.W. Saak, H.M. Jennings, Influence of mixing on the rheology of fresh cement paste, Cement and Concrete Research 29 (9) (1999) 1491–1496.
[22] J.C. Tchamba, S. Amziane, G. Ovarlez, N. Roussel, Lateral stress exerted by fresh cement paste on formwork: laboratory experiments, Cement and Concrete Research 38 (4) (2008) 459–466.
[23] N. Roussel, A thixotropy model for fresh fluid concretes: theory, validation and applications, Cement and Concrete Research 36 (10) (2006) 1797–1806.
[24] J. Assaad, K.H. Khayat, H. Mesbah, Variation of formwork pressure with thixotropy of self-consolidating concrete, ACI Materials Journal 100 (1) (2003) 29–37.
[25] R. Buscall, The elastic properties of structured dispersions: a simple centrifuge method of examination, Colloids and Surfaces 5 (4) (1982) 269–283.
[26] I.M. Krieger, T.J. Dougherty, A mechanism for non-Newtonian flow in suspensions of rigid spheres, Journal of Rheology 3 (1) (1959) 137–152.
[27] L. Struble, G.K. Sun, Viscosity of Portland cement paste as a function of concentration, Advanced Cement Based Materials 2 (1995) 62–69.
[28] R.C. Ball, P. Richmond, Dynamics of colloidal dispersions, Physics and Chemistry of Liquids 9 (2) (1980) 99–116.
[29] S. Mansoutre, P. Colombet, H. Van Damme, Water retention and granular rheological behavior of fresh C_3S paste as a function of concentration, Cement and Concrete Research 29 (9) (1999) 1441–1453.
[30] J.Z.Q. Zhou, T. Fang, G. Luo, P.H.T. Uhlherr, Yield stress and maximum packing fraction of concentrated suspensions, Rheologica Acta 34 (6) (1995) 544–561.

[31] C.R. Wildemuth, M.C. Williams, Viscosity of suspensions modeled with a shear-dependent maximum packing fraction, Rheologica Acta 23 (6) (1984) 627–635.
[32] H.M. Wyss, E.V. Tervoort, L.J. Gauckler, Mechanics and microstructures of concentrated particle gels, Journal of the American Ceramics Society 88 (9) (2005) 2337–2348.
[33] M.D. Green, M. Eberl, K.A. Landman, Compressive yield stress of flocculated suspensions: determination via experiment, American Institute of Chemical Engineering Journal 42 (8) (1996) 2308–2318.
[34] K.T. Miller, W. Shi, L.J. Struble, C.F. Zukoski, Compressive yield stress of cement paste, Materials Research Society Symposium Proceedings 370 (1995) 285–291.
[35] Active Minerals Company LLC, What is Acti-Gel® 208 and how is it made?, 2007.
[36] Stephan Schmidte Gruppe, Technisches Datenblatt Concresol® 105, 2004 in German.
[37] Engelhard, MetaMax® high-reactivity metakolin for concrete, 2008.
[38] T.C. Papanastasiou, Flows of materials with yield, Journal of Rheology 31 (5) (1987) 385–404.
[39] P.D.A. Mills, J.W. Goodwin, B.W. Grover, Shear field modification of strongly flocculated suspensions — aggregate morphology, Colloid and Polymer Science 269 (9) (1991) 949–963.
[40] P.J. Andersen, The effect of superplasticizers and air-entraining agents on the zeta potential of cement particles, Cement and Concrete Research 16 (6) (1986) 931–940.
[41] J.A. Lewis, H. Matsuyama, G. Kriby, S. Morissette, J.F. Young, Polyelectrolyte effects on the rheological properties of concentrated cement suspensions, Journal of the American Ceramics Society 83 (8) (2000) 1905–1913.
[42] A.M. Kjeldsen, R.J. Flatt, L. Bergström, Relating the molecular structure of comb-type superplastizers to the compression rheology of MgO suspensions, Cement and Concrete Research 36 (7) (2006) 1231–1239.
[43] K.T. Miller, R.M. Melant, C.F. Zukoski, Comparison of the compressive yield response of aggregated suspensions: pressure filtration, centrifugation, and osmotic consolidation, Journal of the American Ceramic Society 79 (10) (1996) 2545–2556.
[44] C.F. Ferraris, K.H. Obla, R. Hill, The influence of mineral admixtures on the rheology of cement paste and concrete, Cement and Concrete Research 31 (2) (2001) 245–255.
[45] F. Lange, N. Mörtel, V. Rudert, Dense packing of cement pastes and resulting consequences on mortar properties, Cement and Concrete Research 27 (10) (1997) 1481–1488.
[46] V.S. Ramachandran, Concrete Admixtures Handbook, Properties, Science and Technology, Noyes Publications, Park Ridge, NJ, 1995.
[47] B. Li, X. Wu, Influence of fly ash and its mean particle size on certain engineering properties of cement composite mortars, Cement and Concrete Research 35 (6) (2005) 1128–1134.
[48] S. Wei, Y. Handong, Z. Binggen, Analysis of mechanisms on water-reducing effect of fine ground slag, high-calcium fly ash and low-calcium fly ash, Cement and Concrete Research 33 (8) (2003) 1119–1125.